Parametric exploration of vertical tapered coupler for 3D optical interconnection

Romain Schuster, Alberto Parini, Gaetano Bellanca

Parametric exploration of vertical tapered coupler for 3D optical interconnection

Romain Schuster
Telecom Bretagne, Campus Brest,
655 Avenue du Technopole
29280 Plouzané, Brest, France
romain.schuster@telecom-bretagne.eu

Alberto Parini
FOTON Laboratory, CNRS
University of Rennes 1, ENSSAT
F-22305 Lannion, France
alberto.parini@univ-rennes1.fr

Gaetano Bellanca
Department of Engineering,
University of Ferrara,
Via Saragat 1, 44122 Ferrara, Italy
gaetano.bellanca@unife.it

***Abstract*—In this paper, we numerically investigate tapered waveguide couplers for vertical interconnection. Three different platforms enabling 3D stacking of optical circuitry are considered: crystalline silicon over crystalline silicon, amorphous silicon over crystalline silicon and silicon nitride over crystalline silicon. The performance in terms of insertion loss are evaluated and discussed.**

Keywords—3D stacking; optical vertical links; inverse tapers; insertion loss; finite difference time domain

I. INTRODUCTION

In the last years, electronic-photonic convergence is emerging as an effective approach to overcome the limits, determined by bandwidth bottleneck and high power consumption, on the integration scalability of electrically interconnected networks. Optical interconnections, in fact, can provide a huge communication bandwidth and a favorable power budget with respect to the electrical counterpart.

Silicon is the ideal platform for the integration with CMOS transistors of optical components. Up to now, the most popular approach for this integration has been a coplanar design of functional silicon devices on a silicon-on-insulator substrate. However, the increase in device density, with the unavoidable raise of the number of waveguide crossings, calls for an alternative solution based on a 3D integration approach. Waveguide crossings, indeed, reduce the performance of the system, as they introduce attenuation for scattering and possible unwanted coupling. Optical amplifiers can compensate the attenuation, but are ineffective for the power penalty determined by the crosstalk.

Efficient routing of optical signals among different vertical links requires design and fabrication of low-loss vertical waveguide couplers. Several solutions have been proposed so far for practical implementations, namely: Multi Mode Interference (MMI) structures [1], coupled gratings [2], silicon-nitride micro-ring based links [3, 4] and tapered couplers [1, 5].

In this work, we numerically investigate the performance of 3D vertical couplers based on inverse tapers operating for the fundamental TE mode of optical waveguides located on two different layers. The coupling structure is similar to the one described in [5]; however, three different platforms are considered. The first one is a crystalline silicon over crystalline silicon adhesively bonded as in [6]. In the second platform, amorphous silicon over crystalline silicon waveguides separated by silica are used [5]. The last solution, on the contrary, relies on silicon nitride over crystalline silicon waveguides [7].

In the first section, the main properties of the three investigated technological platforms are shortly described. Then, a configuration with a perpendicular crossing of two waveguides located on different optical layers is analyzed through FDTD simulations, with the aim to evaluate the insertion loss as a function of the distance between the two waveguide layers. This allows to identify, for each investigated platform, the minimum value of the gap compatible with a predefined value of the losses caused by the intersection of waveguides fabricated on two different layers.

Once determined the minimum value of the gap, different vertical coupler configurations have been simulated. Results are presented in Section IV. The worst case corresponding to a 3D stacking of silicon waveguide with silicon-nitride is analyzed in more detail, and then optimized. Discussions and conclusions are drawn at the end.

II. TECHNOLOGICAL PLATFORMS FOR 3D STACKING

The three investigated platforms have been often proposed in literature, and measurements on fabricated devices confirm the validity of these approaches for the implementation of 3D integration of optics at chip level. A sketch with a short description of the different configurations is illustrated in Fig. 1.

The main properties of these platforms can be summarized as follows:

Platform A: Adhesively Bonded Silicon Nanomembranes

In this configuration, which has been recently proposed [6], two crystalline silicon nanomembranes (c-Si), both deriving from standard SOI chips, are bonded one over the other by exploiting the adhesively properties of a SU8 polymer layer (see Fig. 1). On such a structure, a 1-to-32 H-tree optical network for clock distribution has been successfully fabricated and characterized [5]. The refractive index of crystalline silicon is $n_{Si} = 3.45$, whereas the refractive index of SU8 is $n_{SU8} = 1.575$. Authors of [5] measured a propagation loss value of 4.3 dB/cm for structures fabricated on the bonded top layer, against a propagation loss value in the order of 2.5÷3 dB/cm for a classical crystalline SOI waveguide.

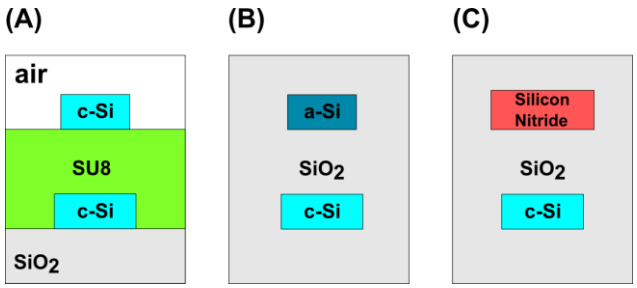

Figure 1: Schematic representation of the three considered technological platforms. (A) Top and bottom guiding layers are made of crystalline silicon (c-Si) with an interposed layer of SU8 polymer. (B) The waveguide on the bottom is made of crystalline silicon, while the silicon oxide and the top guiding layer are in amorphous silicon (a-Si), being both fabricated via chemical deposition. (C) In this case, the top guiding layer is made with silicon nitride deposited above amorphous silica. The waveguide on the bottom is on crystalline silicon.

Platform B: Amorphous Silicon over Crystalline Silicon

Here, a second top guiding layer of amorphous silicon (a-Si) is chemically deposited over a standard SOI substrate. As for the previous platform, the guiding layer on the bottom is made with crystalline silicon (c-Si). This technological platform has been proposed in [6], where vertical couplers with inverse tapers have been fabricated and characterized. The refractive index of the amorphous silicon is $n_{Si} = 3.7$, whereas the refractive index of silica is $n_{SiO2} = 1.45$. Propagation losses for amorphous silicon waveguides are generally larger than 3 dB/cm [7].

Platform C: Silicon Nitride over Crystalline Silicon

In this third solution, the top guiding layer is fabricated through deposition of silicon nitride on the top of a standard SOI substrate [8]; therefore, this is a hybrid platform. As before, the guiding layer on the bottom is made with crystalline silicon (c-Si). The refractive index of silicon nitride is $n_{Si3N4} = 2.0$. Propagation losses for silicon nitride waveguides obtained by deposition are of about 1 dB/cm [9].

We initially focus our activity on the exploration of these three platforms, in order to obtain suitable designs for waveguides operating in single TE mode at telecom wavelengths (1550 nm). To this purpose, we used a finite difference modal solver [10]; the waveguide design parameters (geometry and effective index of the fundamental TE mode) are reported in Table I.

TABLE I. WAVEGUIDE PROPERTIES

Waveguide Core Material	**Waveguide properties**		
	Waveguide width (nm)	***Waveguide height (nm)***	***Effective Index fundamental mode @ 1550nm***
c-Si $n_{SI} = 3.45$	480	220	2.389
a-Si $n_{SI} = 3.77$	480	220	2.736
Si_3N_4 $n_{Si3N4} = 2.0$	1000	400	1.642

III. DESIGN OF THE VERTICAL LAYER STRUCTURE

Isolation between layers on 3D stacking is fundamental to avoid crosstalk and insertion loss. The scenario of Fig. 2, where two waveguides located on different optical layers cross (but do not intersect) orthogonally, has therefore been initially considered and investigated through FDTD simulations [11]. In this scenario, the propagating field of each waveguide is perturbed by the presence of the adjacent guiding structure; the perturbation depends both on the distance *g* and on the shape of the guided modes at the working wavelengths. In fact, a mode that occupies a wide area around its guiding core is strongly affected by the perturbation introduced by any inhomogeneity in the surrounding environment. Mode confinement is heavily correlated to the geometry of the waveguide and to the effective index which, in turn, depends on the wavelength: the closer the effective index to the refractive index of the waveguide core, the higher is the mode confinement.

The mutual interference between waveguides on the crossing has been evaluated by comparing the power at each waveguide output with the corresponding input power. Taking Fig. 2 as a reference, we defined:

$$\begin{aligned} IL_{LOW} &= -10 \cdot \log_{10}(P_2 / P_1) \\ IL_{UP} &= -10 \cdot \log_{10}(P_4 / P_3) \end{aligned} . \qquad (1)$$

These quantities respectively represent the insertion loss for the bottom (IL_{LOW}) and the top (IL_{UP}) waveguides.

For each technological platform the worst case scenario, which corresponds to propagation in the waveguide with the smaller effective index, has been considered. In fact, in this case the mode is less confined inside the core, and is more subject to scattering losses due to perturbations determined by the presence of the other waveguide structure.

As one can observe in Fig. 3, for platforms (A) and (B) the insertion loss is quite similar; in these cases, a gap of 400 nm can guarantee losses smaller than 0.05 dB. For the hybrid platform (C) on the contrary, due to the lower confinement of the Si_3N_4 waveguide, a gap $g = 1000$ nm is required to achieve an insertion loss below 0.15 dB.

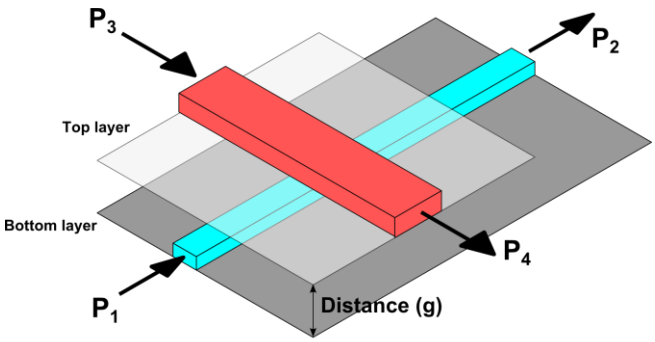

Figure 2: Sketch of the crossing between waveguides on two different optical levels used to evaluate the minimum value of the gap *g* allowing a predefined amount of insertion loss.

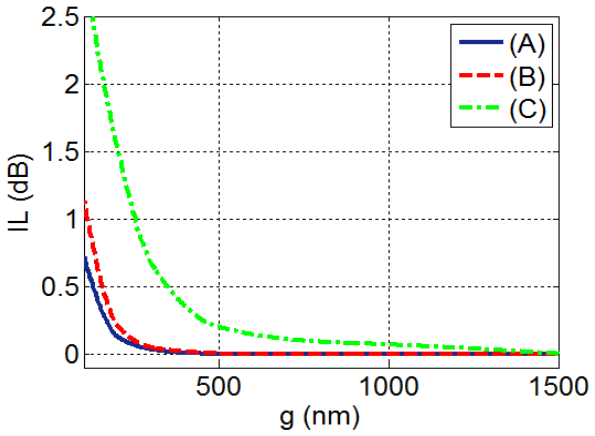

Figure 3: Insertion Loss (IL) of the crossing illustrated in Fig. 2 as a function of the vertical distance between the layers (*g*). The solid blue line refers to the technological platform (A), whereas the red dashed one is for the platform (B). In both cases, the propagation is considered in the bottom silicon crystalline waveguide, and the upper waveguide is the perturbing structure. For the case (C), on the contrary, the propagation is on the upper structure (less confined mode). Insertion loss is described by the green dash-dotted curve. The working wavelength is $\lambda = 1550$ nm.

In this configuration, where waveguides crosses orthogonally, the crosstalk (coupling between waveguides on different layers) is always lower than -10 dB, and can be safely neglected.

IV. Design of the Vertical Coupler

A schematic representation of the vertical coupler with inverse tapers is illustrated in Fig. 4. Reasons for using this configuration are well explained in reference [5]. Our purpose here is to investigate the performance of this coupler for different technological platforms, and to suggest some possible optimizations.

The transmission efficiency can be evaluated through the power budget between the upper and the lower layers:

$$IL_{Link} = -10 \cdot \log_{10}\left(Pout_{UP} / Pin_{LOW}\right) \qquad (2)$$

The parameters for the design are the taper lengths, respectively Lt_{UP} and Lt_{LOW}, and their reciprocal shift with respect to the complete superimposition along the propagation direction.

We initially determined the insertion loss as a function of the taper lengths when the two tapers are completely superimposed. We used a gap $g = 400$ nm, which is suitable for both the (A) and (B) platforms (losses < 0.05 dB). In both of these platforms, the waveguides have the same geometry and quite similar effective indexes; therefore, we considered tapers of the same lengths.

Fig. 5 shows the FDTD calculated insertion loss as a function of the taper lengths for a wavelength $\lambda = 1550$ nm. As one can observe, for lengths above the limit $Lt_{UP} = Lt_{LOW} = 50$ μm, the relationship between insertion loss and taper length is almost linear. Moreover, for tapers 100 μm long, the insertion loss of the vertical coupler is negligible.

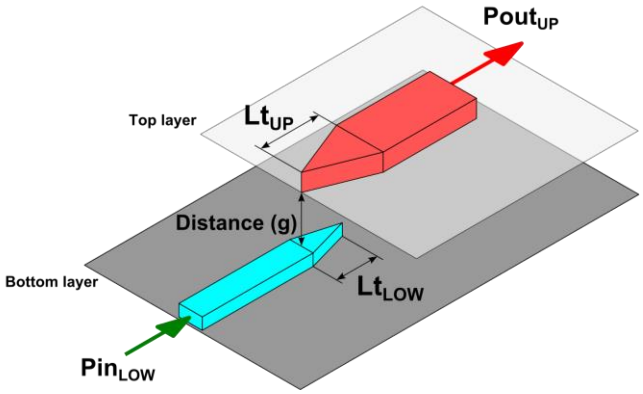

Figure 4: Sketch of the vertical link between optical waveguides on different layers separated by a distance *g*. Inverse tapers are used to ease both the design procedure and the fabrication process.

This configuration can therefore be used for both (A) and (B) platforms. The same amount of insertion loss is obtained also for the platform (C). In this case, however, we expect a quite high amount of insertion loss when waveguides on different levels crosses, as indicate by the plot of Fig. 3 (green dash-dotted curve). In fact, for this platform the gap *g* between the two layers should be increased.

For the platform (C) it is interesting to consider the dependence of the insertion loss of the vertical coupler on the distance between the two layers, which is shown in Fig. 6. As one can note, losses increase with the distance *g*. For a gap $g = 1000$ nm, as needed by this platform to have an insertion loss in orthogonal crossings of 0.15 dB (see Section III), the vertical coupler is unacceptable lossy: tapers do not work in an optimal configuration. Increase in performance can be obtained by progressively shifting the tapers one respect to the other, as illustrated in Fig. 7. In this figure, the curve reports the insertion loss as a function of the longitudinal shift of the tapers, the zero shift corresponding to complete superimposition. As one can observe, the performance increases significantly when the tapers are suitably positioned.

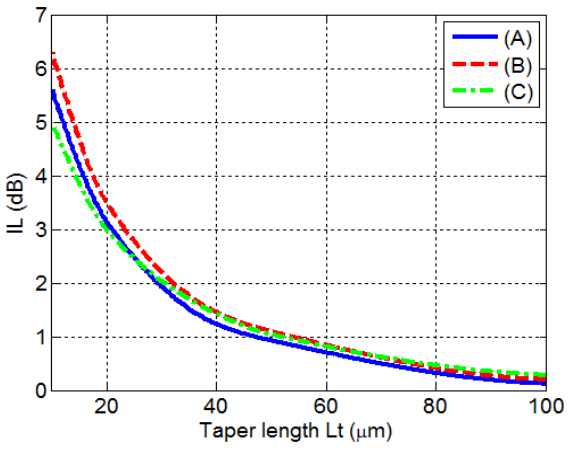

Figure 5: Insertion loss as a function of the taper length for the three platforms; the gap is $g = 400$ nm. For taper lengths above 50 μm, the relation between insertion loss and taper length is almost linear in all the investigated platforms. The working wavelength is $\lambda = 1550$ nm.

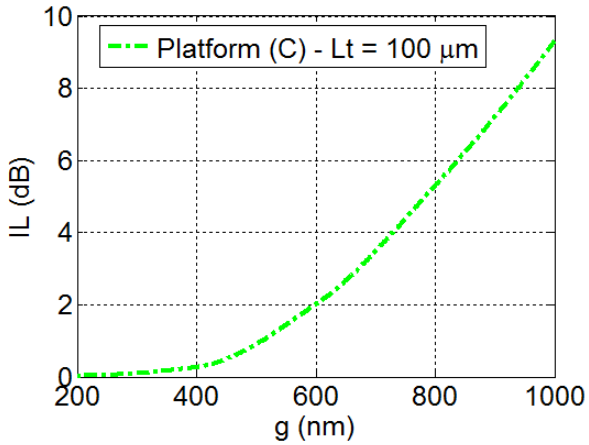

Figure 6: Insertion loss of a vertical tapered link fabricated on the platform (C) with taper length Lt = 100 µm and for λ = 1550 nm. The distance *g* between the layers is progressively increased from 200 nm to 1000 nm. As the distance increases, the insertion loss grows with an almost quadratic trend.

With an optimized shift of about 40 µm, the simulated insertion loss drops to 2.3 dB.

This optimized design of a vertical coupler can be exploited for the fabrication of a hybrid two level optical layer, which allows avoiding multiple crossings with a sequence of parallel running waveguides [12]. By supposing a reference optimized planar crossing with 0.2 dB loss with a footprint of 20 µm, and a vertical optimized coupler with an insertion loss of 2.3 dB (as the one previously outlined for the platform C), the two level bridge becomes a suitable option when more than 24 consecutive crossings could be avoided. If less performing planar crossings are considered (for example crossings with an insertion loss of 0.7 dB), the bridge is already attractive when removing more than 7 crossings. In these computations, losses due to the propagation in the straight waveguide sections have been neglected, due to their low value with respect to crossing and to vertical link losses.

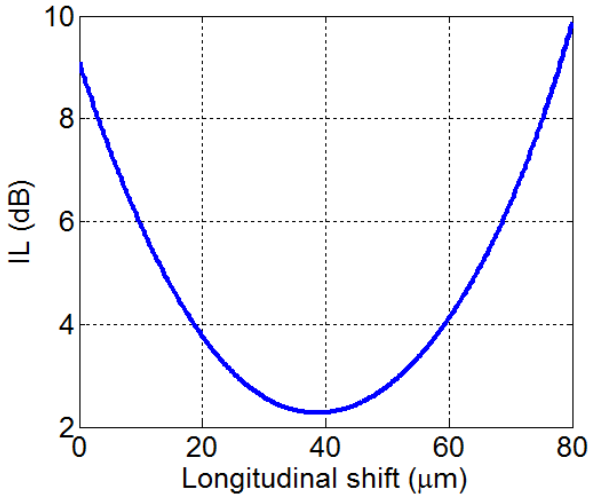

Figure 7: Insertion loss as a function of the longitudinal shift of the two tapers for λ = 1550 nm. The gap between the two waveguide layers is 1000 nm. The optimized longitudinal shift is of about 40 µm; the corresponding insertion loss is 2.3 dB.

V. Conclusions

In this work, we investigate the performance of vertically tapered couplers in three different technological platforms: crystalline silicon over crystalline silicon, amorphous silicon over crystalline silicon and silicon nitride over crystalline silicon. The distance between waveguide layers has been determined first, in order to avoid insertion loss in waveguide crossing. For platforms with strong confining waveguides, as the ones with silicon on both layers, a gap $g = 400$ nm guarantees small insertion loss in crossing. On the contrary, the hybrid platform with silicon nitride needs gaps of the order of 1000 nm. For all the platforms, when a small gap is used, a taper length of 100 µm allows vertical coupling with insertion loss smaller than 0.3 dB. On the contrary, for the platform with silicon nitride waveguide on the top, where a gap $g = 1000$nm is needed, the insertion loss is greater than 9 dB. However, the structure can be optimized by introducing a longitudinal shift between the tapers. In this case, the insertion loss is smaller than 2.5 dB. With this optimized design, the use of a second optical layer becomes suitable when avoiding more than 24 optimized planar crossings.

Acknowledgment

Alberto Parini thanks the "*3D-Optical-ManyCores*" Project, supported by the CominLabs Excellence Laboratory, as well as the Brittany Region (France).

References

[1] A. Parini, G.Calò, G. Bellanca, V. Petruzzelli, "Vertical link solutions for multilayer optical-networks-on-chip topologies," Optical and Quantum Electronics, Volume 46, Issue 3, pp. 385-396, (2014).

[2] M. Sodagar, R. Pourabolghasem, A.A. Eftekhar, A. Adibi, "High-efficiency and wideband interlayer grating couplers in multilayer Si/SiO2/SiN platform for 3D integration of optical functionalities," Optics Express 16777, Vol. 22, No. 14, (2014)

[3] N. Sherwood-Droz, M. Lipson, "Scalable 3D dense integration of photonics on bulk silicon," Optics Express 17758, Vol. 19, No. 18, (2011).

[4] A. Biberman et al., "Photonic network-on-chip architectures using multilayer deposited silicon materials for high-performance chip multiprocessors,". ACM J. Emerg. Technol. Comput. Syst. 7, 2, (2011).

[5] Y. Zhang, X. Xu, D. Kwong, J. Covey, A. Hosseini, R.T. Chen, "0.88 THz Skew-free 1-to-32 Optical Clock Distribution on Adhesively Bonded Silicon Nanomembrane," IEEE PTL, Vol. 26, No. 23, (2014).

[6] R. Sung et al., "Impedance matching vertical optical waveguide couplers for dense high index contrast circuits," Optics Express 11684, Vol. 16, No. 16, (2008).

[7] Timo Lipka, Melanie Kiepsch, Hoc Khiem Trieu, and Jorg Muller "Hydrogenated amorphous silicon photonic device trimming by UV-irradiation," Optics Express 22, No. 10, (2014).

[8] A.M. Jones, C.T. DeRose, A.L. Lentine, D.C. Trotter, A.L. Starbuck, R.A. Norwood, "Ultra-low crosstalk, CMOS compatible waveguide crossings for densely integrated photonic interconnection networks," Optics Express 12002, Vol. 21, No. 10, (2013).

[9] N. Sherwood-Droz, M. Lipson, "Scalable 3D dense integration of photonics on bulk silicon," Optics Express 17758, Vol. 19, No. 18, (2011).

[10] A. B. Fallahkhair, K. S. Li and T. E. Murphy, "Vector Finite Difference Modesolver for Anisotropic Dielectric Waveguides," J. Lightwave Technol., 26 (11), 1423-1431, (2008).

[11] http://www.lumerical.com/tcad-products/fdtd/.

[12] A.M. Jones et al., "Layer separation optimization in CMOS compatible multilayer optical networks," Optical Interconnects Conference, 2013 IEEE, pp. 62,63, (2013).